Surface & Coatings Technology 484 (2024) 130880

Contents lists available at ScienceDirect

Surface & Coatings Technology

journal homepage: www.elsevier.com/locate/surfcoat

Metallization of polypropylene substrates through surface functionalization and physical vapor deposition of chromium coatings

Nicholas Fumagalli [a], Juan Carlos de Haro Sanchez [a], Claudia Letizia Bianchi [b], Stefano Turri [a], Gianmarco Griffini [a,*]

[a] Department of Chemistry, Materials and Chemical Engineering "Giulio Natta", Politecnico di Milano, Piazza Leonardo da Vinci 32, 20133 Milano, Italy
[b] Department of Chemistry, Università degli Studi di Milano, Via Golgi 19, 20133 Milano, Italy

ARTICLE INFO

Keywords:
Polypropylene
Physical vapor deposition
Adhesion
Chromium
Metal on plastics
UV-photografting

ABSTRACT

Physical vapor deposition (PVD) of chromium coatings represents an interesting alternative to electroplating to obtain metallized plastic parts for a variety of manufacturing sectors. This process is however hampered by the limited adhesion of the metallic layer on the underlying polymeric substrates. Within this context, PVD metallization of polypropylene substrates has so far been particularly challenging given the low surface energy and poor wettability of this commodity plastics. To address this issue, a comprehensive approach is proposed here to enable the production of PVD-metallized PP substrates with excellent and stable interlayer adhesion. The adhesive properties of the PP substrate are modified by a selective UV-induced photografting process in which vinyl-, glycidyl- or 2-hydroxyethyl methacrylate species are covalently attached to the PP surface, as confirmed by Fourier-transform infrared spectroscopy, X-ray photoelectron spectroscopy and surface wettability measurements. Based on the chemistry of the photografted functionality, different resin systems are selected and investigated for use as primers to enable subsequent chromium deposition, including acrylic, epoxy and polyurethane systems. The effect of the photografting process on the adhesion between PP and the primers is systematically assessed by means of pull-off tests, highlighting a significant improvement of the adhesion force after surface functionalization with appropriate grafting agents. Finally, functionalized PP substrates are chromated through PVD, obtaining homogeneous and crack-free chromium surfaces upon judicious selection of suitable primer-grafting agent combinations. This also led to outstanding interlayer adhesion and micromechanical performance. This work provides the first demonstration of chromium-metallization of PP substrates *via* PVD for metallized plastic components with excellent surface characteristics, and paves the path for the design of mechanically durable and aesthetically-compliant PVD-metallized PP components.

1. Introduction

The metallization of plastic substrates is a widely used finishing technology in many manufacturing sectors, including automotive, energy, packaging, electronics, and design products [1]. Indeed, despite having advantageous properties (*i.e.*, corrosion resistance, lightness, easy processing), polymeric materials lack in performance under certain conditions, including poor electrical conductivity, low wear resistance and high sensitivity to light [1,2]. Thus, the introduction of a suitable metallic coating layer helps in overcoming these limitations when the polymer component is in use. Nowadays, one of the most widely used metallization technologies to obtain surface-hard plastics is based on the combination of an electroless plating treatment to make the substrate conductive, followed by electroplating, in the presence of hexavalent chromium - Cr(VI). The resulting metallic (typically chromated) coatings are known for their high resistance to wear and very good adhesion. Nevertheless, the significant environmental and safety concerns combined with the regulatory constraints for these plating processes have spurred the exploration of more sustainable alternatives [3–5]. The reasons for these concerns are associated to the galvanic baths on which this process is based on: Cr coatings are usually deposited by means of electrolytes containing chromium trioxide (CrO_3), which can react to form an aqueous solution of chromic acid (H_2CrO_4) when in contact with water [6]. During this process, mists and aerosols of this electrolyte are generated yielding emissions of Cr(VI), which is known to be responsible for chronic poisoning by direct contact with skin or by inhalation [7,8].

* Corresponding author.
E-mail address: gianmarco.griffini@polimi.it (G. Griffini).

https://doi.org/10.1016/j.surfcoat.2024.130880
Received 31 October 2023; Received in revised form 16 April 2024; Accepted 2 May 2024
Available online 3 May 2024

Galvanic baths based on the less toxic trivalent chromium have been proposed as safer option, but with application mainly in the decorative field. [9–11]

A potential alternative to this technology for the deposition of thin layers of metals like chromium, especially on non-conductive polymeric substrates, is represented by physical vapor deposition (PVD) [12–14]. This is a family of film deposition techniques in which the coating is allowed to grow atom by atom on the target substrate as a result of different processes. In some of the most common variants of this technology, the material to be deposited, usually in a solid or liquid form, is either evaporated by an electric heater or sputtered by the generation of a plasma between the substrate and the coating species, in both cases working under appropriate vacuum conditions [14]. Particularly, PVD sputtering stands out for its coating homogeneity and controlled morphology, low processing temperatures, and more environment-friendly overall process conditions [12,15,16].

In the reference literature, many examples of PVD metallization of polymeric substrates have been reported [17–21], such as the case of acrylonitrile butadiene styrene (ABS) for the automotive sector and for electromagnetic shielding [22,23], polycarbonate (PC) for optical applications [24,25], and polyoxymethylene (POM) for gearings [26,27].

Nonetheless, one of the main issues encountered in PVD process, and in all the plastic metallization methods proposed as alternatives to plating, is the poor adhesion of the resulting metallic coatings on the polymeric substrate materials [1,28]. Indeed, the intrinsic characteristics of low wettability and non-polarity of most of the polymeric surfaces usually require a suitable pre-conditioning strategy and the use of an intermediate coating, typically referred to as primer or base coat. This latter is a layer of material that shows better interfacial adhesion to the polymer, enhancing the final performance of the coated part. A typical cycle to improve the surface adhesion of plastic parts includes a plasma-assisted cleaning/activation, followed by the primer deposition and, finally, by the application of the metallic deposit. The choice of plasma processes as pre-conditioning step is convenient as they provide high levels of polymer etching and increased surface roughness by ion sputtering, in a synergistic manner [28].

However, in the case of polyolefins, and particularly for polypropylene (PP), this cycle is not able to guarantee a sufficiently high adhesion strength of the metallic coating. Indeed, PP shows high inertness due to its non-polar nature. This leads to a low surface energy and wettability, making it difficult for deposits to exhibit high adhesion onto its surface, especially in the case of metals [29].

One possible approach to overcome this issue is to perform a functionalization process of the PP surface, typically by means of UV-assisted grafting polymerization. In this respect, a few works have appeared in the literature regarding this general chemical activation strategy, developed through different ways depending on the chemical functionality to be surface-grafted. Balart et al. worked on PP surface modification by photografting acrylic acid [30] or methyl methacrylate [31,32]. In both cases, a successful increase of the overall surface energy was observed as a result of a gain in its polar component, because of the addition of pendant highly polar groups onto the topmost layer of the underlying substrate. Moreover, a study of the mechanical properties of PP-PP joints using a polyurethane (PU) interlayer adhesive was performed using both shear and T-peel tests. In all cases, the functionalization of the surface of PP was able to guarantee the formation of a strong and stable adhesion joint, leading to a combined adhesive-cohesive fracture type as inferred by scanning electron microscopy (SEM) images.

Pantoja and coworkers [33] studied the effects of a tetraethoxysilane (TEOS) coating on improving the adhesion of plasma-treated PP substrates. Contact angle measurements, X-ray photoelectron spectroscopy (XPS) and Fourier-transform infrared (FTIR) analyses were performed to assess the successful formation of a thin silane layer onto the surface of PP treated by atmospheric air plasma torch (APPT). By means of single lap shear tests, an increase of four times in the shear strength was observed for joints between silanized PP coupons bonded by a single component PU adhesive compared to the same joints only treated with APPT. Finally, Chen et al. [34] worked on the improvement of the long-term stability of the hydrophilic character of PP surface resulting from Ar-plasma pre-conditioning treatment, developing a UV-induced graft polymerization process in which acrylamide (AAm) monomer was deposited and polymerized onto PP fabrics. After an optimization study of process parameters, a stable increase in water absorption was successfully demonstrated. PP fabric samples were immersed in water and the weight variations were measured after defined periods of time. The introduction of covalently-linked permanent polar groups led to a high and stable hydrophilicity for up to seven days of storage, with a water absorption ratio of 500 % for AAm-grafted PP compared to the Ar-plasma treated counterpart.

Based on these recent literature works, a systematic investigation of the effect of different chemical functionalization processes on the wettability and adhesion properties of PP substrates is still lacking. More importantly, no examples have appeared to date in the literature on the development of a complete process to obtain PVD-metallized PP substrates with suitable interlayer adhesion leveraging the concept of chemical photografting.

To bridge this gap, in this work a holistic approach is presented to enable the production of PVD-metallized PP substrates with excellent and stable interlayer adhesion. The adhesive properties of the PP substrate are enhanced by UV-photografting of different methacrylate species onto the surface of PP (*i.e.*, vinyl methacrylate (VMA), glycidyl methacrylate (GMA), and 2-hydroxyethyl methacrylate (HEMA)) and by the selection of suitable resins to be used as primers, in line with the chemistry of the photografted functionality. This strategy allows to obtain metallized plastic components exhibiting excellent interlayer adhesion and significantly greater mechanical durability with respect to conventional PVD-metallized PP surfaces. The chemically functionalized samples were fully characterized and their chemical-physical behavior was compared with the pristine and plasma-treated-only counterparts to assess the successful photografting polymerization process in altering their surface properties. Upon primer deposition and chromium metallization *via* PVD, the multi-layer materials were tested by means of pull-off testing to gain quantitative insights into the enhancement in adhesive strength as a result of the proposed pre-conditioning strategy.

2. Materials and methods

2.1. Materials

PP substrates (Moplen HP500 N) were supplied by LyondellBasell. Different methacrylates (vinyl methacrylate - VMA, glycidyl methacrylate - GMA, and 2-hydroxyethyl methacrylate - HEMA), the photoinitiator benzophenone (BP), and the monomers for the synthesis of the acrylic and the epoxy resins (1,6-hexanediol diacrylate - HDDA, pentaerythritol tetraacrylate - PETA, tris[2-(acryloyloxy)ethyl] isocyanurate - TAEI and 3,4-epoxycyclohexylmethyl-3′,4′-epoxycyclohexane carboxylate – ECC) were purchased from Sigma-Aldrich and used without any further purification. The aromatic polyisocyanate based on toluene diisocyanate (TDI) Desmodur L 75 and the saturated polyester polyol Novasynt 17VA596 (OH number: 115 mg KOH/g and acid number: <2 mg KOH/g) were generously provided by Covestro AG and Novaresine srl, respectively. The photoinitiators ethyl phenyl(2,4,6-trimethylbenzoyl) phosphinate (Omnirad TPO-L) and 4,4′-dimethyl-diphenyl iodonium hexafluorophosphate (Omnicat 440) were obtained from IGM Resins.

2.2. Experimental methods

2.2.1. Plasma treatment

The plasma was excited by an inductive-coupled radio frequency

generator at 13.56 MHz. The system contained a mass flow controller for oxygen gas inlet, a pressure gauge, a vacuum pump, and a radio frequency source. Before introduction in the plasma reactor chamber, PP substrates were washed with water and soap to remove any contamination and dust, rinsed with water, and dried under N_2 stream. PP substrates were then plasma-treated for 15 min at a power of 180 W.

2.2.2. Photo-grafting

The methacrylic compounds used as grafting agents (*i.e.*, VMA, GMA, HEMA) were dissolved in acetone at a volume ratio 1:4 v/v under stirring. After the homogenization of the solution, BP was added (5 wt% with respect to the weight of the methacrylate). After the plasma treatment, a given amount of grafting solution containing the photoinitiator was deposited in air on the PP substrate.

To create a thin layer of liquid (~500 μm), a quartz window was placed on top of photografting solution under mild pressure. Then, the assembled unit was irradiated under UV-A light (high-pressure mercury vapor lamp type Zs by Helios Italquartz, with emittance in the 315–400 nm range and a power intensity of ~80 mW/cm^2) from the top at room temperature for 15 min. After that, the covering quartz window was removed, the samples were washed with acetone and distilled water to remove non-grafted chemicals, and finally dried at room temperature under a nitrogen flux before further characterization.

2.2.3. Primer preparation, deposition and curing

The primer based on acrylic resin was formulated by blending HDDA, TAEI and PETA in a 40:40:20 weight ratio, followed by the addition of 4 wt% Omnirad TPO-L as radical UV-photoinitiator. The primer based on epoxy resin was prepared using ECC as only monomer, adding 2 wt% of cationic photoinitiator Ominicat 440. The primer based on the urethane resin was formulated by mixing suitable amounts of saturated polyester polyol (Novasynt 17VA596) and polyisocyanate (Desmodur L 75) in order to obtain a OH:NCO molar ratio equal to 1.

The so-obtained primer precursors were deposited onto PP substrates by means of spin-coating to obtain a final thickness of the cured material of ~15 μm (optical profilometry). To that end, different spin-coating speeds were investigated so as to calibrate the deposition process for each resin system (Fig. S1 in the Supporting Information).

In order to achieve full curing of the primer layer on the PP substrates, different procedures were used as a result of the different chemical nature of the systems. For UV-crosslinkable resins (*i.e.*, acrylic and epoxy), photo-calorimetry measurements (UV-DSC) were employed to identify the exposure time required to maximize the conversion of the photocrosslinking reaction, by monitoring the residual enthalpy of reaction for increasing times of UV light irradiation. In the process conditions (room temperature, ~80 mW/cm^2 irradiance), UV-exposure times of 180 s and 300 s were found to be necessary to achieve nearly quantitative (>99 %) crosslinking conversion in acrylic and epoxy primers, respectively (see Fig. S2 in the Supporting Information for the evolution of the extent of crosslinking in the two UV-curable resin systems over UV-irradiation time). For the urethane-based resin, thermal curing was performed according to the resin supplier specifications (*i.e.*, 120 °C for 30 min). This yielded complete crosslinking, as evidenced by solubility tests in tetrahydrofuran (the cured system exhibited gel content >99 %) and by DSC analyses (negligible residual enthalpy of reaction after the curing cycle).

2.2.4. Magnetron sputtering of chromium

Thin films of metallic chromium (Cr) were deposited on the PP substrates *via* magnetron sputtering using a Leybold-Heraeus LH Z400 MS laboratory system. As sputtering conditions, a power of 35 W (*viz.*, a deposition rate of 13 nm/min) for 30 min was selected to obtain a homogeneous Cr layer with a thickness of ~400 nm. The thickness of the obtained Cr layer was determined by means of a surface profiler (KLA Tencor P15).

2.3. Characterization techniques

Differential scanning calorimetry (DSC) was used to investigate the thermal transitions in the cured acrylic, epoxy and urethane-based primers. The measurements were carried out on solid-state samples (~10 mg) by using a Mettler Toledo DSC/823e instrument, performing three runs (heating/cooling/heating) from −50 °C to 200 °C at a scan rate of 20 °C/min under N_2 atmosphere. The determination of the glass transition temperature (T_g) of the tested materials was based on the evaluation of the inflection point of the DSC trace in the last heating ramp. To investigate the crosslinking kinetics of the photocuring process in UV-curable primers based on acrylic and epoxy resins, the same instrument was used for photo-calorimetric analyses, in combination with a medium-pressure mercury lamp (Lightning cure LC8, Hamamatsu), emitting in the 300–450 nm wavelength range. In particular, the extent of crosslink (EC) was evaluated following Eq. 1, where ΔH_{tot} is the enthalpy of reaction measured when the test is performed on the pristine not-crosslinked resin and $\Delta H(t)$ is the residual enthalpy of reaction measured after exposure of the resin to UV light for a time *t*.

$$EC\ (\%) = 1 - \frac{\Delta H(t)}{\Delta H_{tot}} \cdot 100 \quad (1)$$

Fourier-transform infrared (FTIR) spectroscopy was performed on a Nicolet 760 FTIR spectrophotometer. Measurements were performed in attenuated total reflection (ATR) mode at room temperature in air, recording 64 accumulated scans at a resolution of 2 cm^{-1} in the 4000–400 cm^{-1} wavenumber range.

X-ray photoelectron spectroscopy (XPS) measurements were performed on pristine, plasma-treated and UV-photografted PP substrates using a Mprobe apparatus (Surface Science Instruments) equipped with a monochromatic Al K-α radiation (1486.6 eV) source. Survey analysis in the whole range of X-ray spectra and high-resolution analysis in the typical regions of C_{1s} and O_{1s} were registered. The 1s energy level of carbon at 284.6 eV was taken as the internal reference for peak shift correction.

Static optical contact angle (OCA) measurements on PP substrates were performed at room temperature using an OCA 20 (Data Physics) instrument equipped with a CCD photocamera and with a 500 μL Hamilton syringe to dispense liquid droplets. Water (H_2O) e diiodomethane (CH_2I_2) were used as probe liquids. For each probe liquid, around 15 measurements were performed in different regions of each PP substrate and the average value was recorded.

An Olympus BX60 reflected-light optical microscope, coupled with an Infinity 2 digital camera, was used to analyze the surface morphology of chromated PP surfaces.

Microindentation measurements were carried out on bare PP, PP-primer and PP-primer-chromium multilayered substrates using a Fisher Scope HP100V micro-indenter, equipped with a standard diamond Vickers tip, in force-controlled set up. During the tests, samples were loaded from 0 mN to 30 mN during 60 s, maintaining the force at 30 mN for 60 s and then releasing the force at the same rate, while the test force, the corresponding indentation depth and the test time were recorded. At least six measurements were carried out for each substrate in different region of the samples, and the average and standard deviation were then computed.

A FRU-WR10-0 digital colorimeter was used to assess the color coordinates in the CIE (Commission Internationale de l'Eclairage) L*a*b* color space of the PVD chromium layers deposited on treated PP substrates.

The adhesion strength of the primer and the Cr layer on the PP substrates was evaluated with a PosiTest AT-M Manual adhesion pull-off tester (DeFelsko) by measuring the pulling force needed to detach a 20 mm diameter aluminum dolly adhered to the substrate by means of an epoxy adhesive (Araldite 2011, curing cycle: 24 h at 50 °C).

3. Results and discussion

3.1. Surface activation of PP substrates

As alternative to traditional plasma-based surface activation treatments for PP substrates, a photo-induced radical grafting process is proposed in this work using a series of different methacrylic compounds as surface functionalizing agents. One possible chemical mechanism for this surface activation process is schematically represented in Fig. 1. Under the action of UV radiation, radical species are formed from the homolytic dissociation of the photoinitiator BP, thus generating BP· radicals. By interaction with the PP surface, such active species can generate an interlock point *via* H abstraction on nearby PP macromolecules, most likely on the most substituted carbon atoms belonging to the polyolefin main chain (*viz.*, the most stable radical species). In the presence of unsaturated species as grafting agents, this newly generated interlock active center can further react, yielding their chemical grafting on the surface of the PP substrate. Following this process, tailored covalent functionalization on the PP surface could be achieved in this work by grafting different methacrylic compounds (*i.e.*, GMA, HEMA and VMA) *via* a 2-methylpropionate moiety. The so-obtained activated PP substrates were named PP_X, where X represents the methacrylic compound used in the photo-grafting process.

The chemical modifications occurring on the PP surface during the UV-photografting process were evaluated by means of ATR-FTIR spectroscopy (Fig. 2). As can be observed in the spectra, pristine PP only presents the characteristic signals of C—H stretching vibrations in the 3000–2800 cm^{-1} range, the -CH_3 and -CH_2- asymmetric deformation vibrations at 1455 cm^{-1} and the -CH_3 symmetric deformation vibrations at 1377 cm^{-1} [35]. These signals can also be observed in all the activated PP surfaces. After the photo-grafting process, all the spectra showed the signal related to the stretching vibration of C═O groups, originating from the methacrylic moiety. In the case of alkyl esters (PP_GMA and PP_HEMA), the carbonyl signal appeared centered at 1730 cm^{-1} [36,37], while for the vinyl ester species (PP_VMA), this signal is shifted to 1740 cm^{-1}. Also, the C—O stretching vibration of ester groups could be observed at 1275 cm^{-1} for saturated esters and 1260 cm^{-1} for PP_VMA. In addition, the intensity of the region associated with the skeletal vibrations of CH_3 and CH_2 groups (1200–1130 cm^{-1}) was found to increase in all the activated PP surfaces, with slight differences among them due to the presence of different vicinal functional groups. Finally, some other signals related to the incorporation of specific moieties were detected, such as the symmetric stretching vibration of epoxy ring at 910 cm^{-1} for PP_GMA [38], the stretching vibration of O—H groups in the 3700–3550 cm^{-1} region together with the C—O stretching in primary alcohols at 1080 cm^{-1} for PP_HEMA [37], and the stretching vibration of C═C bond in vinyl esters at 1645 cm^{-1} for PP_VMA [39].

XPS analyses were performed on pristine and functionalized PP substrates to better investigate the chemical changes occurring at the surface as a result of the different surface treatments, namely plasma activation only, and plasma activation in combination with photo-grafting in the presence of different methacrylic functionalities. As shown in Fig. 3, the low-resolution survey spectra revealed mainly the presence of core level O_{1s} (532 eV) and C_{1s} (284.6 eV) in all the PP substrates. By dividing the area underneath the two corresponding peaks, the atomic ratio O/C was determined. Notably, the O/C ratio increased from 0.085 to 0.379 after the oxygen plasma treatment, indicating the successful incorporation of oxygenated species on the PP surface. Instead, all UV-photografted PP substrates presented O/C ratios between those of pristine and plasma-treated PP, indicating the presence of more oxygenated species in the functionalized surfaces compared to the pristine material. Indeed, all the grafted species incorporate a common 2-methylpropionate moiety as a result of the photo-grafting reaction.

Since the binding energy of C_{1s} and O_{1s} presents small variations depending on their vicinal atoms and type of bonding, high-resolution XPS analyses were conducted for a further and more detailed characterization on the surface chemistry of the functionalized PP substrates. The high-resolution XPS spectra for all systems are reported in Fig. 4. The experimental data were fitted with a Gaussian function (solid lines) whose deconvolution highlighted the presence of different peaks (dashed lines) associated with the different carbon or oxygen functional groups detected.

The C_{1s} XPS spectrum of untreated PP (Fig. 4A) can be fitted with two peaks at 284.6 eV and 285.5 eV which can be attributed to C-H/C-C and C—O groups, respectively [35,40]. The presence of the latter peak suggests that even the pristine material surface shows some oxidized carbon atoms, likely due to impurities [41]. After air-plasma treatment (Fig. 4B), additional oxidized species appear at higher binding energies. Particularly, peaks associated with carbonyl groups C═O and ester groups O-C═O are found at 286.7 eV and 288.7 eV [35,41]. For what concerns the UV-photografted PP substrates, a general decrease in the peak area (*viz.*, atomic concentration) for signals associated with carbon atoms incorporated within the main polymer chain (*i.e.*, C—C and C—H) is observed in favor of an increasingly more abundant presence of the aforementioned oxidized species. The atomic concentrations of C_{1s} groups calculated from the high-resolution spectra for all samples are reported in Table 1.

High-resolution spectra of O_{1s} confirm the larger presence of oxygenated species for treated PP surfaces. Indeed, the deconvolution of the experimental XPS signal registered for the pristine PP material yields two main peaks centered at ~532 eV and 533 eV (Fig. 4F), which can be assigned to C—O (oxygen single-bonded to aliphatic carbon) and O-C-O (ether functional group), respectively. Such signals can be found in all the XPS spectra of all functionalized PP samples [42,43]. After plasma treatment, an additional peak appears from the core level oxygen XPS analysis, centered at ~534 eV (Fig. 4G). This signal can be assigned to single-bonded oxygen in carboxylic acid or ester groups [44], indicating a higher extent of surface oxidation. As to UV-photografted systems, specific deconvolution peaks assigned to characteristic oxygen local bonding environments can be identified. More specifically, in the PP_GMA spectrum a peak centered at around 533.3 eV can be noticed, which is typically found in epoxidized systems [42]. Similarly, typical signals associated with oxygen in hydroxyl groups are detected in the XPS spectrum of PP_HEMA, as highlighted by the deconvolution signal

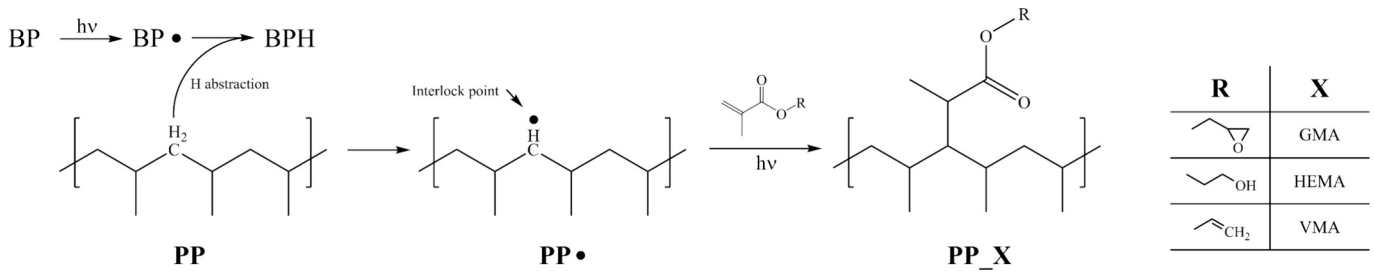

Fig. 1. Process scheme of methacrylate photografting onto PP surface.

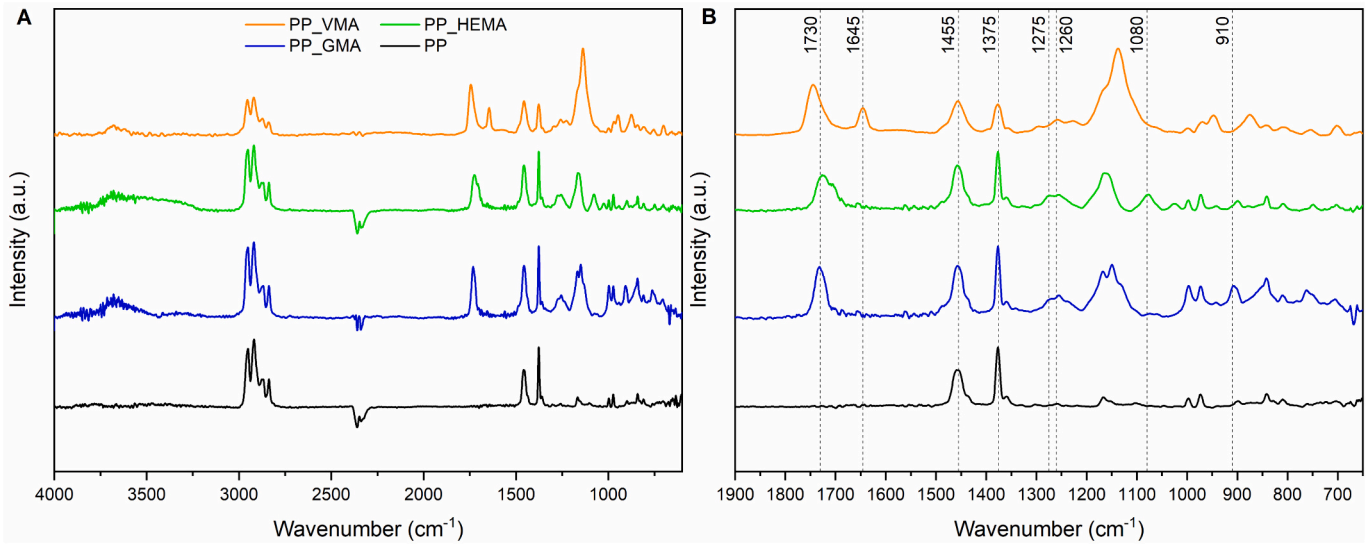

Fig. 2. A) ATR-FTIR spectra of pristine and activated PP surfaces and B) enlarged view of the 1900–650 cm^{-1} spectral region.

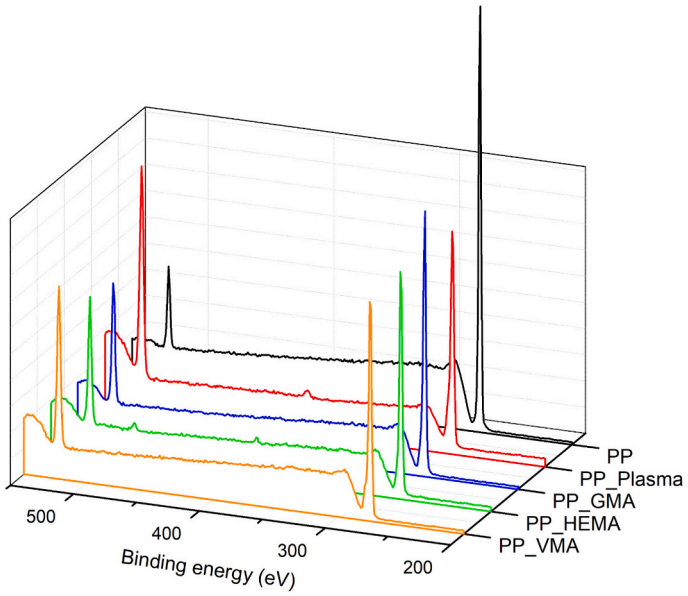

Sample	O/C (atomic ratio)
PP	0.085
PP_Plasma	0.379
PP_GMA	0.201
PP_HEMA	0.245
PP_VMA	0.297

Fig. 3. XPS survey spectra for all the PP substrates, with table indicating the corresponding O/C atomic ratio.

peaking at 530.4 eV [45]. These results provide a direct evidence of the presence on the surface of treated PP substrates of the characteristic functional groups originating from GMA, HEMA and VMA, thereby confirming their successful surface photografting reaction.

The surface wettability properties of the activated PP surfaces were investigated by means of optical contact angle measurements using water (H_2O) and diiodomethane (DIM) as probe liquids. Additionally, the value of surface energy for both pristine and treated PP surfaces was estimated using the Owens, Wendt, Rabel and Kaeble (OWRK) method. The values for water (θ_{H2O}) and diiodomethane (θ_{DIM}) contact angles for all substrates, together with the values of surface tension (γ^{tot}) and corresponding dispersive (γ^{d}) and polar (γ^{p}) components are presented in Table 2. The parent PP exhibited a clear hydrophobic behavior ($\theta_{H2O} = 95.5°$, $\theta_{DIM} = 57.1°$), with a relatively low value for the surface tension $\gamma^{tot} = 30.38$ mN/m, mainly arising from its dispersive component ($\gamma^{d} = 29.05$ mN/m, $\gamma^{p} = 1.33$ mN/m). In the case of PP_VMA, the slightly lower water contact angle ($\theta_{H2O} = 81.3°$) might be attributed to the partial increase in the polarity of the PP surface generated by the incorporation of the methacrylate ester group. Indeed, no major effects are to be expected from the presence of the vinyl terminal functional group (-CH_2=CH_2), given its comparable polarity *vs.* -CH_3 in pristine PP. On the contrary, the hydrophilicity of PP_GMA and PP_HEMA was found to increase further as a result of the presence of pendant moieties of higher polarity ($\theta_{H2O} = 75.1°$ and 57.4° for PP_GMA and PP_HEMA, respectively). Additionally, the surface tension of all the activated PP surfaces was found to be larger than the one reported for untreated PP, further confirming successful chemical modification of the surface and improved surface wettability. It is worth mentioning that optical contact angle measurements were also conducted on plasma-treated PP substrates. However, the wettability with water immediately after this surface treatment was nearly complete ($\theta_{H2O} \approx 0°$), which prevented rigorous estimation of the surface energy in this case.

The stability of the surface treatment on PP substrates was investigated in terms of wettability retention over time, considering its importance on the surface adhesion properties in practical contexts such as that of plastic metallization. Thus, the value of θ_{H2O} on PP_HEMA

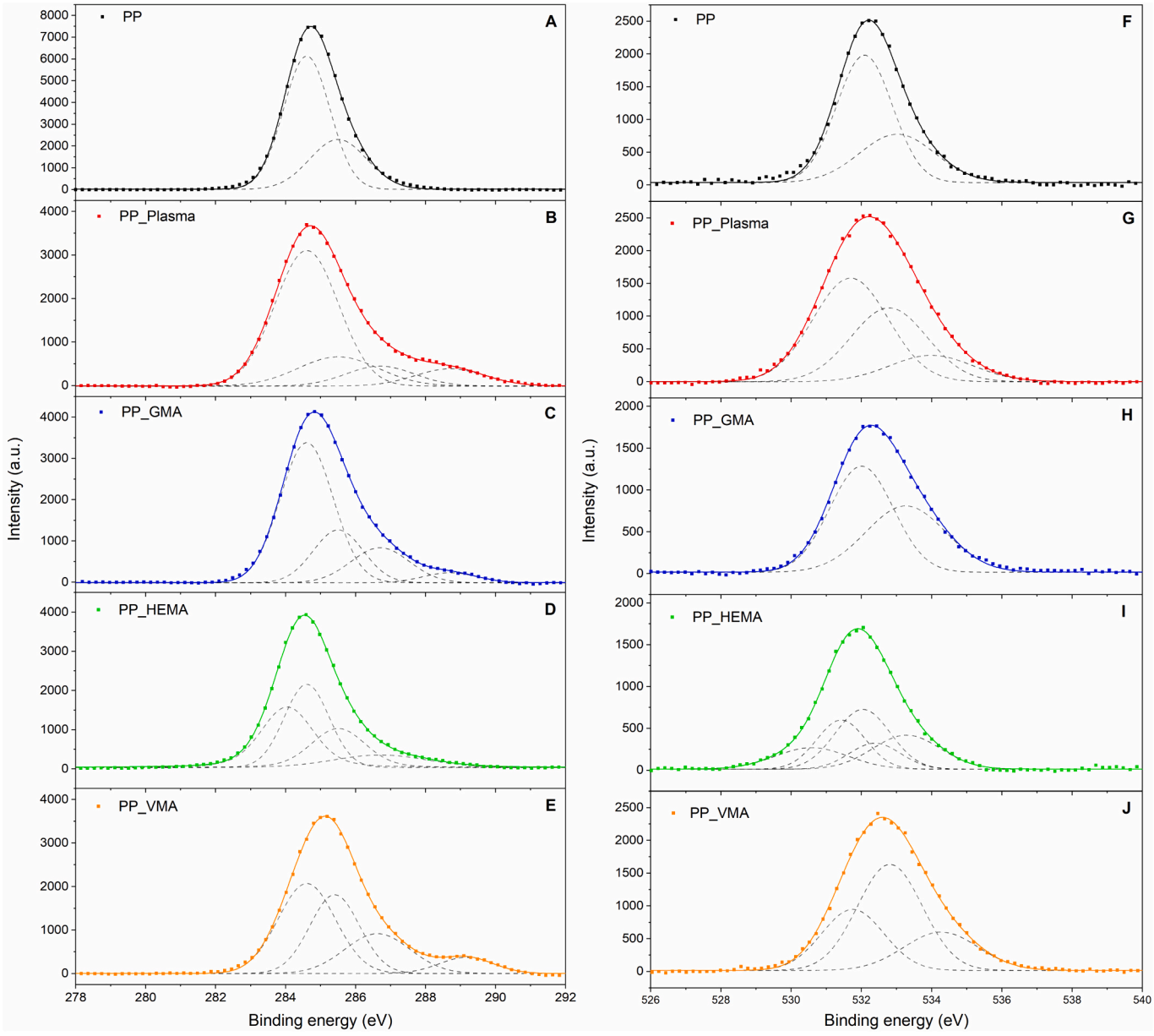

Fig. 4. High-resolution C_{1s} (left) and O_{1s} (right) XPS spectra for (A,F) pristine PP, (B,G) plasma-treated PP, (C,H) PP_GMA, (D,I) PP_HEMA, and (E,J) PP_VMA.

Table 1
XPS C_{1s} groups atomic concentration (%) for all PP surfaces.

Sample	Atomic concentration (%)			
	C-C C-H	C-O C-OH	C=O	O-C=O
PP	77.8	22.2		
PP_Plasma	63.6	17.4	10	9
PP_GMA	58.9	22.8	14.7	3.6
PP_HEMA	67.6	21.2	11.2	
PP_VMA	41	31.2	20.7	7.1

Table 2
Contact angles of water (θ_{H2O}) and diiodomethane (θ_{DIM}), total surface tension (γ_{tot}) and corresponding polar (γ_p) and dispersive (γ_d) components.

Substrate	θ_{H2O} (°)	θ_{DIM} (°)	γ^{tot} (mN/m)	γ^{p} (mN/m)	γ^{d} (mN/m)
PP	95.5 ± 1.3	57.1 ± 1.8	30.38	1.33	29.05
PP_GMA	75.1 ± 1.2	20.7 ± 1.8	49.25	5.29	43.96
PP_HEMA	57.4 ± 1.9	38.3 ± 0.5	47.18	12.61	34.57
PP_VMA	81.3 ± 0.4	45.4 ± 1.3	38.54	5.16	33.37

after surface functionalization was monitored over time during air exposure at room temperature, and compared with that exhibited by PP substrates only treated with air plasma. In particular, PP_HEMA was selected among all UV-grafted PP substrates because of its markedly hydrophilic character (lowest θ_{H2O}), which would provide more evident variations in case of surface wettability modifications. It has been proven in the literature that air plasma treatments on polymeric substrates are characterized by reversible character (hydrophobic recovery), which may be caused by the deactivation of radical species at the surface and the reorientation of hydrophilic groups towards the bulk of the polymer [46]. In line with such observations, PP_Plasma presented a lower contact angle than PP_HEMA during the first 3 h of air exposure, but its hydrophobic recovery was already significant after <24 h and almost complete after 80 h (Fig. 5). On the contrary, PP_HEMA did not show significant variations in θ_{H2O} during this

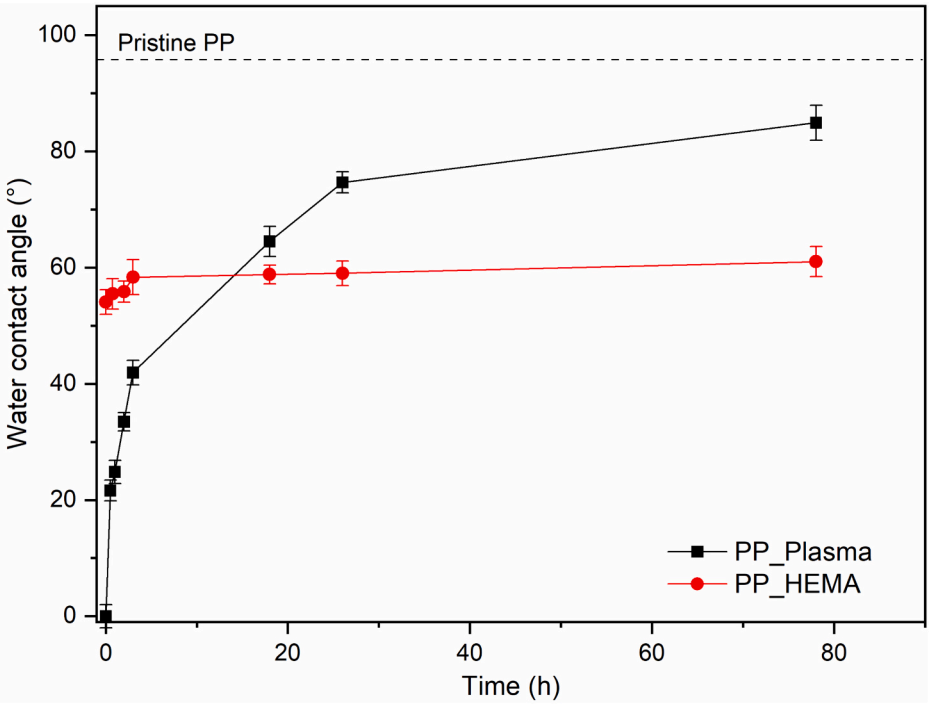

Fig. 5. Comparison of water contact angle on plasma-treated PP and PP_HEMA substrates over time (hydrophobic recovery).

timeframe, confirming the excellent stability of the surface activation. A similar trend was reported by Chen and coworkers [34], in which the water absorption of a plasma-activated PP fabric decayed asymptotically reaching stable values after 4 days meanwhile the one grafted superficially with acrylamide retained the same amount of water after 8 days.

Based on these experimental evidences, the covalent incorporation of the grafting agents on PP substrates can be considered effective for achieving long-term activation of PP, to be further exploited as a tool to enhance the adhesion capacity of different polymeric primers, as will be discussed in the following section.

3.2. Adhesion of primers to PP substrates

In the field of plastic metallization *via* PVD, primers (*i.e.*, polymeric coatings deposited between the underlying substrate and the top metal layer) are usually required to create a homogeneous and non-cracked surface prior to metal deposition. In this work, three different types of primers (namely acrylic, epoxy and urethane) were selected for deposition on both non-activated and activated PP substrates.

Among these primers, those based on acrylic and epoxy chemistries are UV-curable (free-radical *vs.* cationic mechanism, respectively), meanwhile the urethane-based system requires a thermal curing. The combination of a given primer with a specific UV-photografted functional group was selected based on the chemistry of the target system. In particular, the acrylic primer was combined with VMA-grafted substrates, while PP surface functionalization with glycidyl functional groups (GMA) was intended for use with the epoxy primer. Finally, the functionalization with HEMA was designed for the urethane-based system.

The adhesion between the PP substrate and the primer layer is of high interest on these multilayer systems, in order to ensure mechanically durable and aesthetically compliant metallized plastic parts [1,12]. In this respect, the adhesion force of the primers to the functionalized PP substrates was evaluated by means of pull-off tests. The results for all the tested primer-substrate combinations are reported in Table 3.

As benchmark value, the adhesion strength of the primers onto untreated PP substrates was measured. For all the resin systems, an adhesion force of <0.7 MPa was recorded, with full adhesive detachment of the polymeric coating from the substrate on the tested region. This behavior indicates poor adhesive properties on untreated PP, as expected. Upon simple air plasma treatment (PP_Plasma), a slight improvement of the adhesion strength was observed, reaching values between 0.89 MPa and 1.34 MPa depending on the used primer. However, in these cases full detachment of the primer layer was still detected during the adhesion test (Fig. S4 in the Supporting Information). This slight improvement in the adhesion properties in the presence of plasma treatment might be related to the formation of non-covalent interactions between the primer and the substrate, promoted by the formation of oxidized species on the PP surface after plasma exposure, as evidenced by XPS measurements. As opposed to this behavior, the adhesion of the primers on the PP substrates was found to increase significantly after UV-photografting functionalization. In particular, notably higher values of adhesion strength were recorded for all combinations of primer and functionalized substrate. More interestingly, all resin systems led to cohesive mechanical failure of the underlying PP substrate during the pull-off test, clearly indicating excellent primer-substrate interlayer adhesion, higher than the cohesive force of the substrate itself (Fig. S4 in the Supporting Information). The significant improvement of the adhesive properties originating from the UV-photografting functionalization may suggest the formation of covalent bonds at the primer-substrate interface, which are promoted by the favorable interactions between a given grafting agent and a chemically compatible primer.

Table 3
Adhesion strength values for the different primer-substrate combinations.

Primer	Substrate	Adhesion strength (MPa)
Acrylic	PP_Plasma	1.05 ± 0.40
	PP_VMA	1.35 ± 0.16
Epoxy	PP_Plasma	0.89 ± 0.32
	PP_GMA	1.93 ± 0.29
Polyurethane	PP_Plasma	1.34 ± 0.79
	PP_HEMA	3.02 ± 0.72

3.3. Deposition of metallic chromium

Metallic chromium was deposited by PVD on the functionalized PP substrates coated with different primers (*i.e.*, acrylic, epoxy and urethane resins) in order to obtain a final metal layer thickness of ~400 nm as measured by profilometry. Upon visual inspection, the appearance of the metallized layer was found to be influenced by the type and, hence, the characteristics of the underlying primer (Fig. 6). Indeed, chromium deposition on acrylic (Fig. 6A) and epoxy (Fig. 6B) primers yielded a homogeneous and bright metallic layer, with no macroscopic visible defects. On the contrary, deposition on the polyurethane primer led to the formation of visible defects and cracks on the chromium surface (Fig. 6C).

To further assess the aesthetics of the metallic layer on the different substrates, the CIE L*a*b* color space coordinates of the PVD metallic layers were also evaluated. In particular, a slightly lower lightness (L*) for the PP-polyurethane-chromium system (Fig. 6C, inset) was recorded as compared with the other two substrates (Fig. 6A, B), in line with previous considerations.

The different aesthetics of the chromium layer can possibly be related to the thermal transition of the different underlying primers. The acrylic and epoxy resins are characterized by a T_g well above room temperature (Fig. S3 in the Supporting Information). Being in a glassy state, these resins are subjected to low thermal expansions during the PVD deposition process, thus inducing no cracks or defects on the final metallic layer. On the contrary, during the PVD process the polyurethane primer is in its rubbery-leathery state since its T_g is around 20 °C (Fig. S3 in the Supporting Information). The higher thermal expansions typically encountered in these conditions are likely responsible for the formation of heterogeneities of the deposited chromium layer. Indeed, considering the bare primer layers on the corresponding treated PP substrates (Fig. 6D, E, F), no obvious differences on their surface morphology could be detected after deposition. On the contrary, a significantly cracked chromium surface was observed on PP substrates where the polyurethane-based primer was used (Fig. 6I) as opposed to what found with the acrylic (Fig. 6G) and the epoxy (Fig. 6F) primers, in line with previous considerations (additional morphological characterization at the nanoscale through atomic force microscopy can be found in Fig. S5 in the Supporting Information). Based on these evidences, the PP_HEMA/polyurethane primer system was not considered for further characterization.

To assess the surface mechanical response of the PVD chromium coatings, microindentation measurements were conducted on selected substrate-primer-chromium multilayer structures and compared with the results obtained on bare PP and on non-metallized substrate-primer systems. As a result of the previous considerations, only PP_VMA and PP_GMA substrates were considered in combination with the acrylic and the epoxy primers, respectively.

As shown in Table 4, after deposition of the primer, a significant increase in the surface hardness (Vickers hardness, HV) was observed, from 4.38 for bare PP to 84.61 and 79.59 for acrylic and epoxy primer, respectively. This increase was accompanied by an increase in

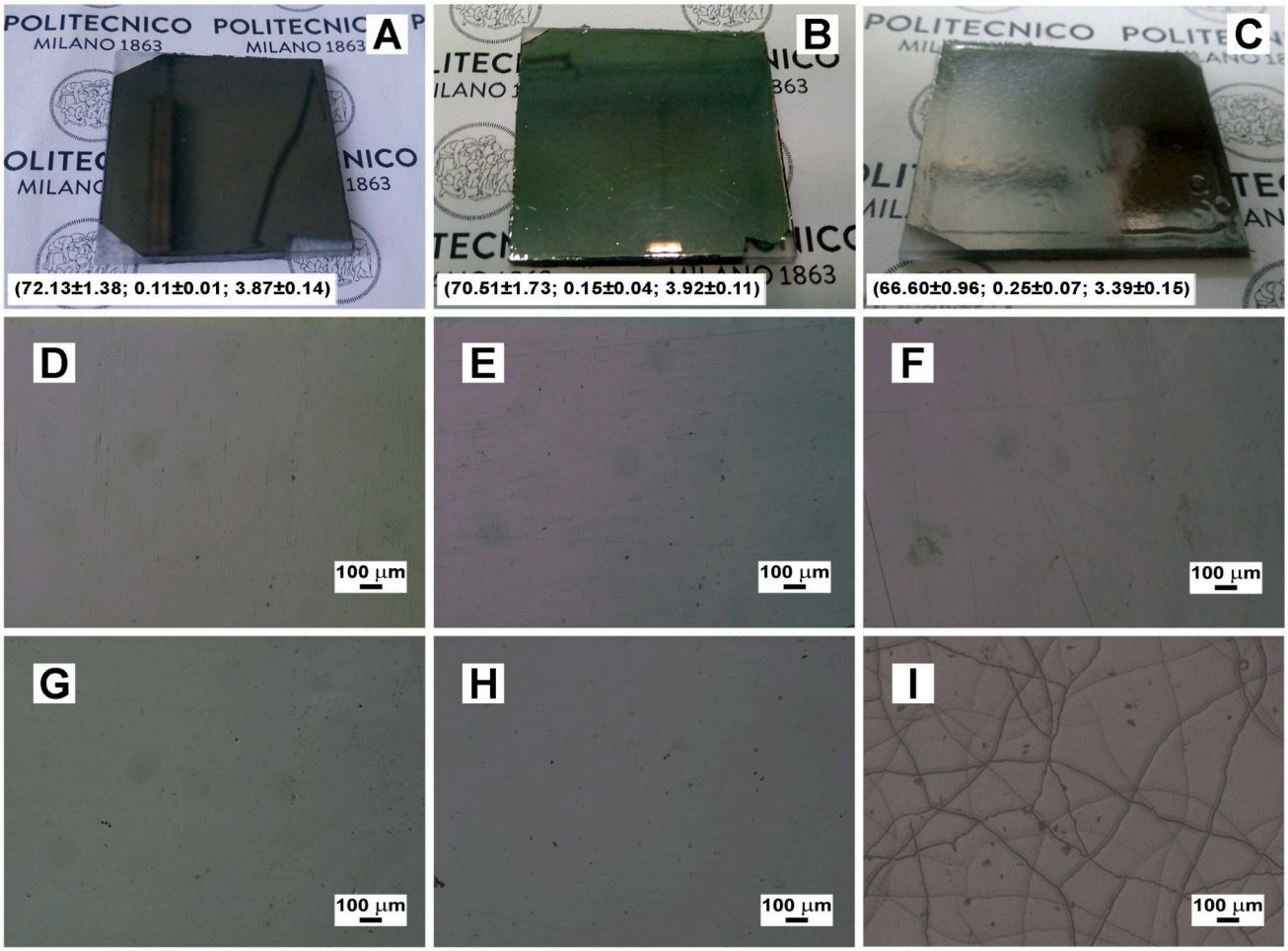

Fig. 6. Photographic images of PP chromated substrates using (A) acrylic, (B) epoxy and (C) polyurethane primers (insets show the CIE L*a*b* color space coordinates, presented as average L*a*b* values ± standard deviation out of 5 measurements). Optical microscopy images of: primer-only coatings (D, acrylic; E, epoxy; F, polyurethane) and of PVD chromium layers deposited on (G) acrylic, (H) epoxy and (I) polyurethane primers on surface functionalized PP substrates.

Table 4
Vickers hardness (HV) and indentation modulus (E_{IT}) for selected substrate-primer and substrate-primer-chromium combinations (mean values and standard deviations out of a minimum of six measurements are reported). When present, the thickness of the chromium layer was ~400 nm, as measured by profilometry.

Substrate	Primer	Chromium	HV (–)	E_{IT} (GPa)
PP	–	–	4.38 ± 0.01	0.83 ± 0.02
PP_VMA	Acrylic	–	84.61 ± 6.01	3.77 ± 0.08
PP_VMA	Acrylic	Yes	603.60 ± 77.37	18.70 ± 0.95
PP_GMA	Epoxy	–	79.59 ± 15.68	3.98 ± 0.23
PP_GMA	Epoxy	Yes	718.99 ± 96.42	19.43 ± 1.14

indentation modulus E_{IT}, from 0.83 GPa in bare PP to ~4 GPa for both substrate-primer combinations. Interestingly, no significant differences were observed between the two primers, thus confirming excellent substrate coverage and successful crosslinking reaction in both cases. The addition of the top PVD chromium layer yielded a further enhancement in the micromechanical response at the surface, leading to HV values in the 600–700 range and E_{IT} values approaching 20 GPa, which are in line or higher than those recently reported for chromium-based (and other metallic) PVD coatings on different polymeric substrates [1,14].

To evaluate the adhesion strength of the metallic coating to the substrate and the overall interlayer adhesion, pull-off tests were performed on the chromated multilayer (substrate-primer-chromium) systems. Firstly, the adhesion of the chromium coating to the underlying primer (acrylic and epoxy) deposited and cured on PP substrates only treated by air plasma was determined, as reference condition. In this case, full detachment of the primer from the substrate was observed, indicating poor primer-substrate adhesion, as expected. The same pull-off test was also performed on chromated multilayers incorporating suitable primer-photografted substrate combinations (acrylic primer on PP_VMA; epoxy primer on PP_GMA). In these cases, a cohesive mechanical failure of the PP substrate was observed (Fig. S6 in the Supporting Information), in analogy to what found in the adhesion tests conducted without the presence of the chromium layer. These results highlight the excellent adhesion of metallic chromium to the underlying layers. This response, combined with the improved interlayer adhesion between primer and functionalized substrate promoted by the presence of covalently linked grafting agents at the PP-primer interface, yields chromated PP parts with enhanced surface and interfacial characteristics.

4. Conclusions

In this work, chemical UV-photografting was employed as successful strategy to obtain PVD-chromated PP substrates with excellent and stable interlayer adhesion. In particular, PP substrates were activated by an air-plasma pre-conditioning treatment followed by selective UV-photografting of vinyl-, glycidyl- or 2-hydroxyethyl methacrylates. Successful covalent surface attachment of these moieties was confirmed by FTIR, XPS and contact angle measurements. Based on the chemistry of the photografted functionality, different resin systems were selected and investigated for use as primers in the multilayer structure, including acrylic, epoxy and polyurethane systems. The effect of the photografting process on the adhesion between PP and the primers was assessed by means of pull-off tests, highlighting a significant improvement of the adhesion force after surface functionalization with appropriate grafting agents, as compared with untreated PP substrates or in the presence of bare air plasma treatment. This behavior was associated with the formation of covalent links at the primer-functionalized substrate interface, which enable favorable chemical interaction and enhanced interlayer bonding. Finally, functionalized PP substrates were chromated by means of PVD, obtaining homogeneous and crack-free chromium surfaces upon judicious selection of suitable primer-grafting agent combinations, which also led to outstanding interlayer adhesion and micromechanical performance.

In conclusion, the novel approach proposed in this study for the metallization of PP substrates enables improved chromium-primer-PP interlayer adhesion for chromated plastic parts with enhanced surface and interface characteristics, and provides useful guidelines for the design of durable and aesthetically-compliant PVD-metallized PP components.

CRediT authorship contribution statement

Nicholas Fumagalli: Formal analysis, Investigation, Writing – original draft. **Juan Carlos de Haro Sanchez:** Data curation, Investigation, Writing – original draft. **Claudia Letizia Bianchi:** Data curation, Investigation, Writing – review & editing. **Stefano Turri:** Conceptualization, Funding acquisition, Supervision, Writing – review & editing. **Gianmarco Griffini:** Conceptualization, Funding acquisition, Supervision, Writing – review & editing.

Declaration of competing interest

The authors declare that they have no known competing financial interests or personal relationships that could have appeared to influence the work reported in this paper.

Data availability

Data will be made available on request.

Acknowledgements

Financial support from Regione Lombardia - POR FESR 2014-2020 (SUPERECOPLAST project, ID: 149049) is greatly acknowledged.

Appendix A. Supplementary data

Supplementary data to this article can be found online at https://doi.org/10.1016/j.surfcoat.2024.130880.

References

[1] R. Melentiev, A. Yudhanto, R. Tao, T. Vuchkov, G. Lubineau, Metallization of polymers and composites: state-of-the-art approaches, Mater. Des. 221 (2022) 110958, https://doi.org/10.1016/j.matdes.2022.110958.
[2] S. Olivera, H.B. Muralidhara, K. Venkatesh, K. Gopalakrishna, C.S. Vivek, Plating on acrylonitrile–butadiene–styrene (ABS) plastic: a review, J. Mater. Sci. 51 (2016) 3657–3674, https://doi.org/10.1007/s10853-015-9668-7.
[3] G. Hong, K.S. Siow, G. Zhiqiang, A.K. Hsieh, A novel chromium plating from trivalent chromium solution, Plat. Surf. Finish. 88 (2000) 69–75.
[4] C. Pellerin, S.M. Booker, Reflections on hexavalent chromium: health hazards of an industrial heavyweight, Environ. Health Perspect. 108 (2000) A402–A407, https://doi.org/10.1289/ehp.108-a402.
[5] R. Saha, R. Nandi, B. Saha, Sources and toxicity of hexavalent chromium, J. Coord. Chem. 64 (2011) 1782–1806, https://doi.org/10.1080/00958972.2011.583646.
[6] D.L. Snyder, Decorative chromium plating basics, Met. Finish. 110 (2012) 14–21, https://doi.org/10.1016/S0026-0576(13)70110-7.
[7] F. Baruthio, Toxic effects of chromium and its compounds, Biol. Trace Elem. Res. 32 (1992) 145–153, https://doi.org/10.1007/BF02784599.
[8] A. Baral, R.D. Engelken, Chromium-based regulations and greening in metal finishing industries in the USA, Environ. Sci. Pol. 5 (2002) 121–133, https://doi.org/10.1016/S1462-9011(02)00028-X.
[9] Giovanardi, G. Orlando, Chromium electrodeposition from Cr(III) aqueous solutions, Surf. Coat. Technol. 205 (2011) 3947–3955, https://doi.org/10.1016/j.surfcoat.2011.02.027.
[10] S. Mahdavi, S.R. Allahkaram, A. Heidarzadeh, Characteristics and properties of Cr coatings electrodeposited from Cr(III) baths, Mater. Res. Express 6 (2019) 026403, https://doi.org/10.1088/2053-1591/aaeb4f.
[11] V.S. Protsenko, Kinetics and mechanism of electrochemical reactions occurring during the chromium electrodeposition from electrolytes based on Cr(III) compounds: a literature review, Reactions 4 (2023) 398–419, https://doi.org/10.3390/reactions4030024.

[12] A. Baptista, F. Silva, J. Porteiro, J. Míguez, G. Pinto, Sputtering physical vapour deposition (PVD) coatings: a critical review on process improvement and market trend demands, Coatings 8 (2018) 402, https://doi.org/10.3390/coatings8110402.
[13] A. Baptista, F. Silva, J. Porteiro, J. Míguez, G. Pinto, L. Fernandes, On the physical vapour deposition (PVD): evolution of magnetron sputtering processes for industrial applications, Procedia Manuf. 17 (2018) 746–757, https://doi.org/10.1016/j.promfg.2018.10.125.
[14] S. Wang, C. Ma, F.C. Walsh, Alternative tribological coatings to electrodeposited hard chromium: a critical review, Trans. Inst. Met. Finish. 98 (2020) 173–185, https://doi.org/10.1080/00202967.2020.1776962.
[15] B. Navinšek, P. Panjan, I. Milošev, PVD coatings as an environmentally clean alternative to electroplating and electroless processes, Surf. Coat. Technol. 116–119 (1999) 476–487, https://doi.org/10.1016/S0257-8972(99)00145-0.
[16] A. Romani, P. Tralli, M. Levi, S. Turri, R. Suriano, Metallization of recycled glass fiber-reinforced polymers processed by UV-assisted 3D printing, Materials (Basel). 15 (2022) 6242, https://doi.org/10.3390/ma15186242.
[17] E. Lugscheider, K. Bobzin, M. Maes, A. Kramer, On the coating of polymers – basic investigations, Thin Solid Films 459 (2004) 313–317, https://doi.org/10.1016/j.tsf.2003.12.134.
[18] E. Woskowicz, M. Łożyńska, A. Kowalik-Klimczak, J. Kacprzyńska-Gołacka, E. Osuch-Słomka, A. Piasek, L. Gradoń, Plasma deposition of antimicrobial coatings based on silver and copper on polypropylene, Polymery 65 (2020) 33–43, https://doi.org/10.14314/polimery.2020.1.5.
[19] P. Sharma, F. Ponte, M.J. Lima, N.M. Figueiredo, J. Ferreira, S. Carvalho, Plasma etching of polycarbonate surfaces for improved adhesion of Cr coatings, Appl. Surf. Sci. 637 (2023) 157903, https://doi.org/10.1016/j.apsusc.2023.157903.
[20] F. Milde, K. Goedicke, M. Fahland, Adhesion behavior of PVD coatings on ECR plasma and ion beam treated polymer films, Thin Solid Films 279 (1996) 169–173, https://doi.org/10.1016/0040-6090(95)08142-9.
[21] C. Kunze, R.H. Brugnara, N. Bagcivan, K. Bobzin, G. Grundmeier, Surface chemistry of PVD (Cr,Al)N coatings deposited by means of direct current and high power pulsed magnetron sputtering, Surf. Interface Anal. 45 (2013) 1884–1892, https://doi.org/10.1002/sia.5336.
[22] J. White, C. Tenore, A. Pavich, R. Scherzer, S. Stagon, Environmentally benign metallization of material extrusion technology 3D printed acrylonitrile butadiene styrene parts using physical vapor deposition, Addit. Manuf. 22 (2018) 279–285, https://doi.org/10.1016/j.addma.2018.05.016.
[23] J.P. Heinß, F. Fietzke, High-rate deposition of thick aluminum coatings on plastic parts for electromagnetic shielding, Surf. Coat. Technol. 385 (2020) 125134, https://doi.org/10.1016/j.surfcoat.2019.125134.
[24] A.A. Ferreira, F.J.G. Silva, A.G. Pinto, V.F.C. Sousa, Characterization of thin chromium coatings produced by PVD sputtering for optical applications, Coatings 11 (2021) 215, https://doi.org/10.3390/coatings11020215.
[25] A. Baptista, G. Pinto, F.J.G. Silva, A.A. Ferreira, A.G. Pinto, V.F.C. Sousa, Wear characterization of chromium pvd coatings on polymeric substrate for automotive optical components, Coatings 11 (2021) 555, https://doi.org/10.3390/coatings11050555.
[26] B. Polanec, F. Zupanič, T. Bončina, F. Tašner, S. Glodež, Experimental investigation of the wear behaviour of coated polymer gears, Polymers (Basel) 13 (2021) 3588, https://doi.org/10.3390/polym13203588.
[27] T. Bončina, B. Polanec, F. Zupanič, S. Glodež, Wear behaviour of multilayer Al-PVD-coated polymer gears, Polymers (Basel). 14 (2022) 4751, https://doi.org/10.3390/polym14214751.
[28] C. Lambaré, P.Y. Tessier, F. Poncin-Epaillard, D. Debarnot, Plasma functionalization and etching for enhancing metal adhesion onto polymeric substrates, RSC Adv. 5 (2015) 62348–62357, https://doi.org/10.1039/C5RA08844E.
[29] C. Zhang, Y. Bai, W. Liu, The approaches for promoting PP adhesion based on the surface modification, J. Adhes. Sci. Technol. 28 (2014) 454–465, https://doi.org/10.1080/01694243.2013.838826.
[30] J. Balart, V. Fombuena, R. Balart, J.M. España, R. Navarro, O. Fenollar, Optimization of adhesion properties of polypropylene by surface modification using acrylic acid photografting, J. Appl. Polym. Sci. 116 (2010) 3256–3264, https://doi.org/10.1002/app.31751.
[31] J. Balart, V. Fombuena, J.M. España, L. Sánchez-Nácher, R. Balart, Improvement of adhesion properties of polypropylene substrates by methyl methacrylate UV photografting surface treatment, Mater. Des. 33 (2012) 1–10, https://doi.org/10.1016/j.matdes.2011.06.069.
[32] J. Balart, V. Fombuena, T. Boronat, M.J. Reig, R. Balart, Surface modification of polypropylene substrates by UV photografting of methyl methacrylate (MMA) for improved surface wettability, J. Mater. Sci. 47 (2012) 2375–2383, https://doi.org/10.1007/s10853-011-6056-9.
[33] M. Pantoja, N. Encinas, J. Abenojar, M.A. Martínez, Effect of tetraethoxysilane coating on the improvement of plasma treated polypropylene adhesion, Appl. Surf. Sci. 280 (2013) 850–857, https://doi.org/10.1016/j.apsusc.2013.05.074.
[34] K.S. Chen, H.R. Lin, S.C. Chen, J.C. Tsai, Y.A. Ku, Long term water adsorption ratio improvement of polypropylene fabric by plasma pre-treatment and graft polymerization, Polym. J. 38 (2006) 905–911, https://doi.org/10.1295/polymj.PJ2005183.
[35] R. Morent, N. De Geyter, C. Leys, L. Gengembre, E. Payen, Comparison between XPS- and FTIR-analysis of plasma-treated polypropylene film surfaces, Surf. Interface Anal. 40 (2008) 597–600, https://doi.org/10.1002/sia.2619.
[36] O.M. Jazani, H. Rastin, K. Formela, A. Hejna, M. Shahbazi, B. Farkiani, M.R. Saeb, An investigation on the role of GMA grafting degree on the efficiency of PET/PP-g-GMA reactive blending: morphology and mechanical properties, Polym. Bull. 74 (2017) 4483–4497, https://doi.org/10.1007/s00289-017-1962-x.
[37] X.M. Xie, N.H. Chen, B.H. Guo, S. Li, Study of multi-monomer melt-grafting onto polypropylene in an extruder, Polym. Int. 49 (2000) 1677–1683, https://doi.org/10.1002/1097-0126(200012)49:12<1677::AID-PI590>3.0.CO;2-0.
[38] M.G. González, J.C. Cabanelas, J. Baselga, Applications of FTIR on epoxy resins - identification, monitoring the curing process, phase separation and water uptake, in: T. Theophanides (Ed.), Infrared Spectroscopy - Materials Science, Engineering and Technology, IntechOpen, 2012, pp. 261–284.
[39] P. Shukla, D. Srivastava, Reaction kinetics of esterification of phenol-cardanol based epoxidized novolac resins and methacrylic acid, Int. J. Plast. Technol. 18 (2014) 1–15, https://doi.org/10.1007/s12588-014-9060-5.
[40] B. Ozkaya, S. Grosse-Kreul, C. Corbella, A. Von Keudell, G. Grundmeier, Combined in situ XPS and UHV-chemical force microscopy (CFM) studies of the plasma induced surface oxidation of polypropylene, Plasma Process. Polym. 11 (2014) 256–262, https://doi.org/10.1002/ppap.201300105.
[41] A. Rjeb, S. Letarte, L. Tajounte, M. Chafik El Idrissi, A. Adnot, D. Roy, Y. Claire, J. Kaloustian, Polypropylene natural aging studied by X-ray photoelectron spectroscopy, J. Electron Spectros. Relat. Phenomena 107 (2000) 221–230, https://doi.org/10.1016/S0368-2048(00)00121-3.
[42] D. Briggs, G. Beamson, XPS studies of the oxygen 1s and 2s levels in a wide range of functional polymers, Anal. Chem. 65 (1993) 1517–1523, https://doi.org/10.1021/ac00059a006.
[43] A. Ganguly, S. Sharma, P. Papakonstantinou, J. Hamilton, Probing the thermal deoxygenation of graphene oxide using high-resolution in situ X-ray-based spectroscopies, J. Phys. Chem. C 115 (2011) 17009–17019, https://doi.org/10.1021/jp203741y.
[44] A. Aarva, V.L. Deringer, S. Sainio, T. Laurila, M.A. Caro, Understanding X-ray spectroscopy of carbonaceous materials by combining experiments, density functional theory, and machine learning. Part II: quantitative fitting of spectra, Chem. Mater. 31 (2019) 9256–9267, https://doi.org/10.1021/acs.chemmater.9b02050.
[45] B. Sivaranjini, R. Mangaiyarkarasi, V. Ganesh, S. Umadevi, Vertical alignment of liquid crystals over a functionalized flexible substrate, Sci. Rep. 8 (2018) 8891, https://doi.org/10.1038/s41598-018-27039-3.
[46] K. Johnsen, S. Kirkhorn, K. Olafsen, K. Redford, A. Stori, Modification of polyolefin surfaces by plasma-induced grafting, J. Appl. Polym. Sci. 59 (1996) 1651–1657, https://doi.org/10.1002/(SICI)1097-4628(19960307)59:10<1651::AID-APP17>3.0.CO;2-Z.